Journal of
Nanoscience and Nanotechnology
Vol. 11, 851–855, 2011

Chemical and Electronic Properties of Ba/Bis(2-methyl-8-quinolinolato)(4-phenylphenolato)Aluminum(III) Interfaces for Organic Light-Emitting Diodes

Jong Tae Lim, Jae Wook Kwon, Jae Beom Park, and Geun Young Yeom*

School of Advanced Materials Science and Engineering, Sungkyunkwan University, Suwon 440-746, Korea

The chemistry, electronic structure, and electron-injecting characteristics at the interfaces that were formed between bis(2-methyl-8-quinolinolato)(4-phenylphenolato)aluminum(III) (BAlq) and barium (Ba) were investigated using ultraviolet photoemission spectroscopy, near-edge X-ray absorption fine structure spectroscopy, X-ray photoemission spectroscopy, and current–voltage–luminance measurements. The device performance of organic light-emitting diodes (OLEDs), which have a glass/ITO/MoO_3/2-TNATA/NPB/BAlq/Ba/Au structure, was significantly improved by inserting a Ba coverage (Θ_{Ba}) of 0.2 nm between BAlq and the cathode. For Θ_{Ba}'s that were thicker than 0.2 nm, however, even though the electron-injecting barrier heights at the Ba-on-BAlq interfaces were all 0.1 eV, the device performance of the OLEDs with Ba at the interface was degraded with increasing Θ_{Ba}. This result indicates that the device performance is largely dependent on the interfacial chemical degradation of the BAlq molecule itself, rather than the electron-injecting barrier height that is determined by the width and chemical structure of the interface, and the formation of barium-induced new gap states at the Ba-on-BAlq interface.

Keywords: Organic Light-Emitting Diode, Electronic Structure, BAlq/Ba Interface.

RESEARCH ARTICLE

1. INTRODUCTION

The organic light-emitting diode (OLED) has attracted considerable attention as one of the most promising next-generation flat panel displays due to its superior performance and potential applications. Since Tang et al. reported an efficient double-layered OLED that utilizes tris(8-quinolinolato)aluminum (III) (Alq_3),[1,2] many aluminum complexes based on quinoline ligands such as q_3Al (q = 8-quinolinolato ligand)[3,4] and q_2AlOR (OR = aryloxy or alkoxy ligand)[5,6] complexes have been developed and have been demonstrated to be useful emissive materials and/or hole-blocking (and exciton-blocking)/electron-transporting materials.[7]

Kwong et al.[8] reported the operating stability and the luminous efficiency of an orange-red phosphorescent OLED with various hole- and exciton-blocking materials of q_2AlOR-type complexes. Among these complexes, the devices that used bis(2-methyl-8-quinolinolato)(4-phenylphenolato)aluminum (III) (BAlq) exhibited the most excellent hole- and exciton-blocking property, which indicated a maximum efficiency of 17.6 cd/A with a projected operational lifetime of 15,000 h, normalized to 100 cd/m^2.[8] Also, the thin film of BAlq in OLED has been widely studied as a blue emissive layer.[9] In addition, as the electron affinity of BAlq is equal to that of Alq_3 (3.0 eV),[10] Alq_3 has been the most widely used electron-transporting layer in OLEDs. The characteristic of an electron-injecting layer for BAlq has not been extensively studied yet, though.

In fact, one of the fundamental issues in optimizing the performance of OLEDs is the need to improve the electron injection through a cathode/organic interface.[11,12] The electron affinities of electron-transporting materials (ETMs) such as Alq_3 and BAlq are much lower than the work function (WF) of typical cathode materials such as Al, Ag and Au.[12] Therefore, they form a high barrier to the electron injection (Φ_B^N)[12,13] at the cathode/ETM interfaces, which leads to high operating voltages and poor long-term stability. The light emission efficiency of OLEDs is limited by the number of injected electrons because most organic semiconductors are *p*-type and their electron mobility is generally slower than their hole mobility. Therefore, an efficient electron-injecting interface is the key to improving the operating voltage and the emission efficiency.[14]

To achieve an efficient electron-injecting interface by lowering the Φ_B^N, lower WF metals such as Cs, Mg, and

*Author to whom correspondence should be addressed.

Ca have been used between the cathode metal and Alq_3.[12] For the cathode/ETM interface, however, not only the energy level alignment at the interface but also the interfacial chemical reaction that can lead to the degradation of the device is an important issue due to the decomposition of the ETM. This interfacial electronic structure that is formed between the ETM and the cathode plays an important role in determining both the luminous efficiency and the lifetime of the devices. In the authors' previous studies,[15] Ba was successfully applied as the electron-injecting interface layer, but the detailed properties of the interfaces that were formed between Ba and BAlq as the electron-injecting interface layers are not yet fully understood. Therefore, in this study, the chemical reaction and the Φ_B^N at the metal-organic interface when Ba was deposited on BAlq were investigated. The correlation between the device performance of the OLEDs and the characteristics of the interface is also discussed in this paper.

2. EXPERIMENTAL DETAILS

The electronic structure of the Ba-on-BAlq interfaces was examined using X-ray photoemission spectroscopy (XPS), ultraviolet photoemission spectroscopy (UPS), and near-edge X-ray absorption fine structure (NEXAFS) spectroscopy at the 4B1 beam line in the Pohang Accelerator Laboratory (Korea). All the measurements and depositions were performed in an ultra-high vacuum system that consisted of a main analysis chamber (approximately $5–10^{-10}$ Torr) and a sample preparation chamber (approximately $5–10^{-9}$ Torr). All the samples were prepared *in-situ* via sequential thermal evaporation on an Si wafer, and their thickness was determined via timed deposition that was calibrated using a quartz-crystal microbalance. In the XPS studies, 650 eV incident photon energy was used for the core level spectra of O 1s and N 1s, and 350 eV was used for Al 2p. For the UPS measurements, the He I (21.2 eV) line from a UV source was used. The photoemission onset that reflected the vacuum level at the surface of all the samples was measured by biasing the samples at −20 V. The incident photon energy was calibrated by measuring the Au 4f level of a clean Au surface. In the NEXAFS analyses, the nitrogen K-edge (387–417 eV) spectra were measured at a photon incident angle of 45°.

The OLEDs were composed of glass/ITO/MoO_3 (5 nm)/4, 4′, 4″-tris(2-naphthylphenyl-1-phenylamino)triphenylamine (2-TNATA, 60 nm)/4,4′-bis(*N*-(1-napthyl)-*N*-phenyl-amino)-biphenyl (NPB, 18 nm)/BAlq (22 nm)/Ba(Θ_{Ba})/Au (100 nm), with Θ_{Ba} values of 0 nm (device 0), 0.2 nm (device 1), 0.4 nm (device 2), and 2.0 nm (device 3). Au was used as a cathode layer to minimize the interaction in the electronic transfer[16] between Ba and the cathode and to prevent a chemical reaction[17] between BAlq and cathode.

All the devices were fabricated via thermal evaporation on glass/ITO substrates. The current density–voltage–luminance characteristics of the devices were measured using a Keithley 2400 electrometer, a photodiode (Oriel 71608), and a Keithley 485 picoammeter.

3. RESULTS AND DISCUSSION

Figure 1 shows the current density–voltage characteristics of devices 0–3. The turn-on voltages (V_T at 0.1 cd/m^2) of devices 1–3 were 3.0, 3.2, and 3.4 V, respectively. Device 0, without Ba, showed a higher V_T value of 6.0 V. The inset of Figure 1 shows the power efficiency (η_{PE}) characteristics as functions of the luminance of devices 1–3. At a luminance of about 100 cd/m^2 (L_{100}), device 1 ($\Theta_{Ba} = 0.2$ nm) showed the highest η_{PE} of 1.6 lm/W. As Θ_{Ba} increased to 0.4 and 2.0 nm, however, η_{PE} decreased to 0.9 and 0.6 lm/W, respectively. These η_{PE} results indicate that the device performance significantly depends on Θ_{Ba}. The device performance was maximized with a 0.2 nm-thick Θ_{Ba} but it deteriorated as Θ_{Ba} exceeded 0.2 nm. To gain further insights on the mechanism involved in the enhancement of the device performance, the Φ_B^N of the Ba-on-BAlq interfaces was investigated as a function of the Θ_{Ba}.

Figure 2(a) shows the spectral region around the highest occupied molecular orbitals (HOMOs) of the Ba-on-BAlq interfaces in the UPS spectra, as a function of the Θ_{Ba} that ranged from 0 to 2.0 nm on BAlq. Also, Figure 2(b) shows the photoemission onset of the UPS spectra that was measured at the Ba-on-BAlq interfaces as a function of the Θ_{Ba} that ranged from 0 to 2.0 nm on BAlq, with a sample bias

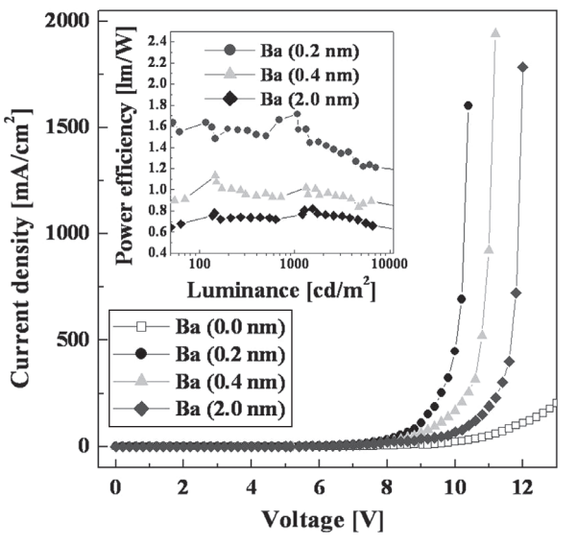

Fig. 1. Current density curves as a function of bias voltage. The inset shows the power efficiency–luminance curves. The devices were composed of glass/ITO/MoO_3 (5 nm)/2-TNATA (60 nm)/NPB (18 nm)/BAlq (22 nm)/Ba (*x* nm)/Al (100 nm). (Ba thickness of devices 0–3 = 0, 0.2, 0.4, and 2.0 nm, respectively).

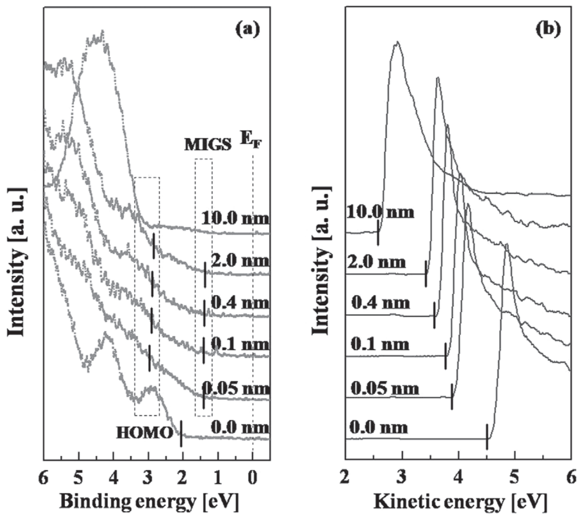

Fig. 2. UPS of the Ba-on-BAlq interface. (a) spectral region around the BAlq HOMO and (b) onset of photoemission with sample bias of −20 V as a function of Θ_{Ba}.

of −20 V, which reflects the WF shifts of BAlq via Ba adsorption. As shown in Figure 2(a), all the BAlq molecular orbital features shifted to a higher binding energy when Θ_{Ba} was above 0.05 nm. In addition, as shown in Figure 2(a), the metal-induced gap state (MIGS),[18] which is roughly a free-electron-like, metal wave function that penetrates the organic semiconductor side, was observed at the forbidden energy gap of approximately 1.4 eV above the HOMO of the Ba-on-BAlq interfaces. The band between BAlq and the cathode was realigned due to the introduced MIGS and the WF difference.[19] In fact, a new gap state was also observed in several interfaces between a low WF metal (e.g., Li, Na, K, Ca, or Mg) and Alq_3.[20] Also, as shown in Figure 2(b), the introduction of Θ_{Ba} on BAlq also shifted the WF to a lower energy level.

Figure 3(a) shows the HOMO level shift ($e_0\Delta V_s = \mathrm{HOMO}_{BAlq} - \mathrm{HOMO}_{Ba\text{-}on\text{-}BAlq}$) and the WF shift ($\Delta\Phi = \Phi_{BAlq} - \Phi_{Ba\text{-}on\text{-}BAlq}$) from Figure 2 for the Θ_{Ba} range of 0.2–2.0 nm. As shown in Figure 3(a), the HOMO level shifted approximately 0.7 eV lower than that of the pure BAlq with the addition of a Θ_{Ba} of about 0.1–2 nm. In the case of Φ_B^N, even though it decreased with the increase in Θ_{Ba}, it decreased by about 0.1 eV for the about 0.1–2 nm Θ_{Ba}, unlike that of the pure BAlq.[11] The HOMO level shifts can be expressed as $e_0\Delta V_s = \Delta I - \Delta\Phi$,[12] wherein ΔI is the ionization energy change. The band bending ($e_0\Delta V_s$) that is marked by the filled squares in Figure 3(a) was not equal to $\Delta\Phi$ ($e_0\Delta V_s \neq \Delta\Phi$), and the definite differences between $e_0\Delta V_s$ and $\Delta\Phi$ indicate that the HOMO-level shift did not simply originate from the WF difference but might have resulted from a possible chemical reaction between BAlq and the cathode. These results suggest that the lowering of the HOMO level at the Ba-on-BAlq interface was not only due to the band bending via the Fermi level pinning, but also due to the chemical modification of the

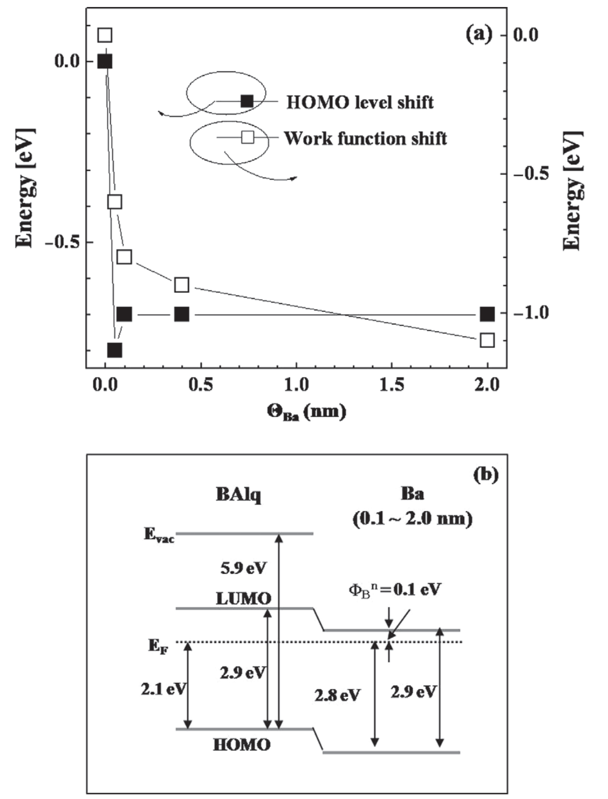

Fig. 3. (a) HOMO level shift [closed squares] of $\mathrm{HOMO}_{BAlq} - \mathrm{HOMO}_{Ba\text{-}on\text{-}BAlq}$ and WF shift [open squares] of $\Phi_{BAlq} - \Phi_{Ba\text{-}on\text{-}BAlq}$ as a function of Θ_{Ba} on BAlq at the pure BAlq and Ba-on-BAlq interface. (b) proposed energy band diagram for BAlq and the Ba-on-BAlq interface when Θ_{Ba} between 0.2 and 2.0 nm is deposited on 10 nm-thick BAlq.

BAlq molecules by the excess electrons of the Ba metal. The presence of MIGS at the Ba-on-BAlq interface, as shown in Figure 2(a), further proves that there was a chemical reaction between Ba and BAlq. Figure 3(b) shows a diagram of the proposed energy band of the Ba-on-BAlq interface at a Θ_{Ba} of 0.1–2.0 nm, as shown in Figure 3(a).[11] Here, the ionization potential and the energy band gap (E_g) of the pure BAlq in Figure 3(a) were 5.9 eV and 2.9 eV, respectively.[10]

Figure 4(a) shows the evolution of the O 1s electron density curves (EDCs) as a function of a 0–2.0 nm Θ_{Ba} on BAlq (100 Å), as measured via XPS. For $\Theta_{Ba} = 0$ Å, the O 1s core-level EDC had a single component, which indicates a clean BAlq film. The single component of the O 1s EDC initially shifted to a higher binding energy of 533.2 eV. The BAlq radical anion was formed via the electron charge transfer (ECT) from Ba until $\Theta_{Ba} =$ 0.2 nm, compared with the pure BAlq of 532.8 eV. At $\Theta_{Ba} = 0.4$ nm, the other O 1s peak at 532.2 eV originated from the decomposition of the Al–O bond breaking that began to appear at the lower binding energy; and at $\Theta_{Ba} = 2.0$ nm, only the O 1s peak at 532.2 eV remained. The peak shift to a lower binding energy was caused by a decrease in the Coulomb potential between

RESEARCH ARTICLE

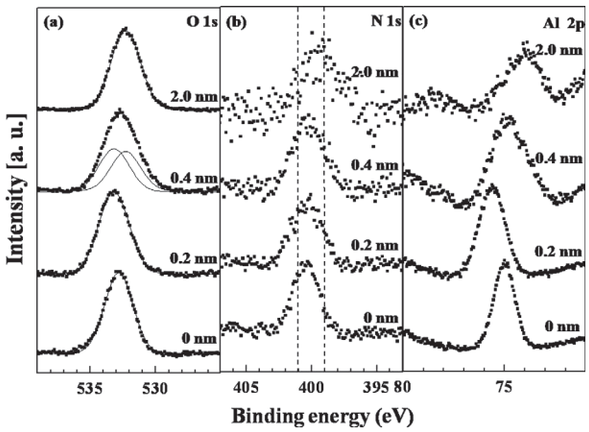

Fig. 4. Evolution of XPS O 1s (a), N 1s (b), and Al 2p (c) core level EDCs as a function of Θ_{Ba} on BAlq. The values in the figures indicate Θ_{Ba}. The peak fitting of O 1s EDC was worked as Ref. [21].

the nuclei and the electrons of the valence band as a result of the increased electron density at the valence band of the O atoms due to the electrons provided by Ba.[11] Choong et al. reported that from the XPS spectra of O 1s, the binding energy difference between an Alq_3 radical component and a decomposition component at the Ca/Alq_3 interface can be estimated, and that it was 2.0 eV.[22] Similarly, in Figure 4(a), the peak shift between the BAlq radical component and the BAlq decomposition component at the Ba-on-BAlq interface was estimated to have been 1.0 eV. This indicates that the Al–O bond breaking could have occurred among the BAlq molecules via the ETC from Ba at a higher Θ_{Ba}.

Figure 4(b) shows the N 1s core-level EDCs as functions of a 0–2.0 nm Θ_{Ba}. Even for the 0.2 nm-thin Θ_{Ba}, a BAlq decomposed component (around 399.0 eV) was observed with the BAlq radical component (around 401 eV). This shows that Ba interacts with N before O, which is reasonable because the Al–N bond is the weakest in the molecule. Considering the dependence of the device characteristics shown in Figure 1 on Θ_{Ba}, the formation of the decomposited component in the N XPS spectra did not affect the device performance at all Θ_{Ba}'s. The emergence of the decomposition component in the O XPS spectra, however, provides a direct cause of the poor device performance at a Θ_{Ba} above 0.4 nm.

Figure 4(c) shows the 2p peaks of Al EDC. The Al 2p peak shifted to the highest binding energy of 75.6 eV at $\Theta_{Ba} = 0.2$ nm. Then the Al 2p peak at which the Θ_{Ba} exceeded 0.2 nm was decomposed into two peaks that were composed of the low-binding energy levels of 73.9 eV and 74.9 eV, respectively.

In the O 1s, N 1s, and Al 2p XPS EDCs, the formation of decomposed BAlq components even at the low Θ_{Ba} of 0.4 nm means a high reactivity between Ba and BAlq at the interface. Unlike this result, the Ba-on-Alq_3 interface and the Ca-on-Alq_3 interface formed a stable Alq_3 radical anion up to $\Theta_{Ba} = 0.4$ nm.[15, 22] The stronger chemical reaction of BAlq than of Alq_3 was due to the molecular structure of BAlq. BAlq, as a q_2AlOR-type complex (q: bidentate ligand, OR: monodentate ligand), and Alq_3, as a q_3Al-type complex, have five- and six-coordinate numbers, respectively. Therefore, when considering an Al atom that is coordinated by ligands, BAlq leads to a higher chemical interaction with Ba than Alq_3, because the ligands in the BAlq molecule do not surround the Al atom as efficiently as those in the Alq_3 molecule.

Figure 5 shows the NEXAFS spectra at the N K-edge of the Ba-on-BAlq interfaces at 0–2.0 nm Θ_{Ba}. The NEXAFS spectroscopy showed the resonance features that were induced by the transition from the initial state (core level) to the final state (vacant level), and that can be used to obtain information on the unoccupied state. The pure BAlq peak due to the transitions of electrons from the N 1s level to LUMO was estimated as about 398.0 eV. Interestingly, a new resonance peak appeared at 391.2 eV upon Ba adsorption. The peaks at 391.2 and 398.0 eV, which were induced by the transition to the LUMO levels that consisted of π^* unoccupied states, are attributed to π^*_{rea} (the species of the N atom that reacted with Ba) and π^*_{unrea} (the species of the N atom that did not react with Ba), respectively. The difference (7.6 eV) in the large photon energy between π^*_{rea} and π^*_{unrea} could be interpreted as having been caused by the change in the final state, such as by the effect of an electron-donating Ba or an excitonic effect[23] during the transition processes, because the N 1s core level did not show any strong feature related to the chemical modification, as shown in Figure 4(b). The appearance of

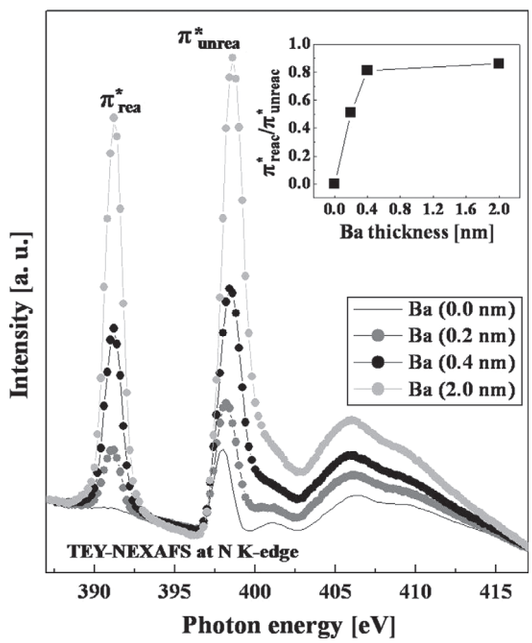

Fig. 5. TEY-NEXAFS spectra at the N K-edge of the Ba-on-BAlq interface for the Θ_{Ba} from 0 to 2.0 nm. The inset shows the intensity ratios for $\pi^*_{rea}/\pi^*_{unrea}$ as a function of Θ_{Ba} between 0 and 2.0 nm.

RESEARCH ARTICLE

a π^*_{rea} peak even at the 0.2 nm Θ_{Ba} on BAlq indicates that the orbitals that were involved with ECT were mainly localized at the pyridyl ring rather than at the phenoxide ring on the 8-quinolinolato ligand that comprised the BAlq molecule.[24]

The inset in Figure 5 shows the effect of ETC for Θ_{Ba} onto Alq_3 in the N K-edge NEXAFS spectra. The intensity ratios of $\pi^*_{rea}/\pi^*_{unrea}$ increased from 0.51 to 0.83 as Θ_{Ba} increased from 0.2 to 2.0 nm. The increase in the π^*_{rea} component with increasing Θ_{Ba} coincides with the trend of the N 1s XPS spectra shown in Figure 2(b).

4. CONCLUSION

The chemistry, electronic structure, and electron-injecting characteristics at the interfaces that were formed between bis(2-methyl-8-quinolinolato)(4-phenylphenolato) aluminum (III) (BAlq) and barium (Ba) were investigated by analyzing the electronic structure and current–voltage–luminance curves. The mechanism involved in the improved device performance that was achieved by incorporating Ba in the cathode structure was investigated. At the Θ_{Ba} of 0.2–2.0 nm, the device performance was enhanced by the lowering of the HOMO level by 0.7 eV, as shown in the UPS spectra. This lowering was due to the MIGS that was formed by a chemical reaction and the band bending that was formed by the Fermi level pinning between Ba and BAlq. Although the Φ^N_B values at 0.2 nm and 2.0 nm Θ_{Ba} were almost identical, the interface chemistry significantly depended on Θ_{Ba}, as shown in the MIGS and the reactive species in the N K-edge NEXAFS spectra. The formation of a stable radical anion at $\Theta_{Ba} = 0.2$ nm enhanced the device performance of the OLED, but the appearance of the Alq_3 decomposed component for $\Theta_{Ba} \geq 0.4$ nm degraded the device performance due to the Al–O bond breaking, rather than the Al–N bond breaking at the Ba-on-BAlq interface.

Acknowledgment: This study was supported by the WCU program of the Korean Science and Engineering Foundation, which is being funded by the Korean government (MOEHRD, Grant No. R32-2008-000-10124-0).

References and Notes

1. C. W. Tang and S. A. Vanslyke, *Appl. Phys. Lett.* 51, 913 (**1987**).
2. J. H. Burroughes, D. D. C. Bradley, A. R. Brown, R. N. Marks, K. Mackay, R. H. Friend, P. L. Burn, and A. B. Homes, *Nature* 347, 539 (**1990**).
3. L. S. Sapochak, A. Padmaperuma, N. Washton, F. Endrino, G. T. Schmett, J. Mrshall, D. Fogarty, P. E. Burrows, and S. R. Forrest, *J. Am. Chem. Soc.* 123, 6300 (**2001**).
4. J. Kido and Y. Lizumi, *Appl. Phys. Lett.* 73, 2721 (**1998**).
5. P. S. Bryran, F. V. Lovecchio, and S. A. VanSlyke, U.S. Patent No. 5141671, August (**1992**).
6. T.-Y. Chu, Y.-S. Wu, J.-F. Chen, and C. H. Chen, *Chem. Phys. Lett.* 404, 121 (**2005**).
7. J. H. Park, J. H. Seo, J. H. Seo, S. J. Lee, J. R. Koo, S. S. Yoon, S. H. Lee, and Y. K. Kim, *J. Nanosci. Nanotechnol.* 8, 4607 (**2008**).
8. R. C. Kwong, M. R. Nugent, L. Michalski, T. Ngo, K. Rajan, Y.-J. Tung, M. S. Weaver, T. X. Zhou, M. Hack, M. E. Thompson, S. R. Forrest, and J. J. Brown, *Appl. Phys. Lett.* 81, 162 (**2002**).
9. T. Tsuji, S. Kawami, S. Miyaguchi, T. Naijo, T. Yuki, S. Matsuo, and H. Miyazaki, *SID Symposium Digest of Technical Papers*, Society for Information Display, Washington, May (**2004**), Vol. 35, p. 900.
10. C. Qiu, Z. Xie, H. Chen, B. Z. Tang, M. W. Wong, and H.-S. Kwok, *IEEE J. Sel. Top. Quantum Electronics* 10, 101 (**2004**).
11. L.-L. Chua, J. Zaumseil, J.-F. Chang, Eric C.-W. Ou, Peter K.-H. Ho, H. Sirringhaus, and R. H. Friend, *Nature* 434, 194 (**2005**).
12. H. Ishii, K. Sugiyama, E. Ito, and K. Seki, *Adv. Mater.* 11, 605 (**1999**).
13. L. S. Lai, M. K. Fung, S. N. Bao, S. W. Tong, M. Y. Chan, C. S. Lee, and S. T. Lee, *Chem. Phys. Lett.* 367, 753 (**2003**).
14. L. C. Palilis, M. Uchida, and Z. H. Kafafi, *IEEE J. Sel. Top. Quantum Electronics* 10, 1 (**2004**).
15. J. T. Lim, K. N. Kim, and G. Y. Yeom, *J. Nanosci. Nanotechnol.* 9, 7485 (**2009**).
16. S. L. Lai, M. K. Fung, S. N. Bao, S. W. Tong, M. Y. Chan, C. S. Lee, and S. T. Lee, *Chem. Phys. Lett.* 367, 753 (**2003**).
17. J.-G. Lee, S. Kim, and K. Jeong, *Appl. Phys. Lett.* 79, 4595 (**2001**).
18. M. Kiguchi, R. Arita, G. Yoshikawa, Y. Tanida, S. Ikeda, S. Entani, I. Nakai, H. Kondoh, K. Saiki, and H. Aoki, *Phys. Rev.* 72, 75446 (**2005**).
19. J. Tersoff, *Phys. Rev. Lett.* 52, 465 (**1984**).
20. C. Shen, I. G. Hill, A. Kahn, and I. Schwartz, *J. Am. Chem. Soc.* 122, 5391 (**2000**).
21. The O 1s core level peak that was acquired from the pristine BAlq layer was fitted by a single Gaussian peak with 2.14 eV of FWHM (full-width half-maximum). All the O 1s spectra from the Ba-adsorbed BAlq surfaces were fitted by Gaussian peaks with FWHMs that were identical to that of the pristine BAlq, i.e., fixed at FWHM = 2.14 eV. The FWHM of the O 1s peak from the Ba 0.4 nm/BAlq surface was fitted to 2.6 eV, however, which was much wider than that of the pristine BAlq, and which indicates an additional chemical environment of oxygen atoms.
22. V.-E. Choong, M. E. Mason, C. W. Tang, and Y. Gao, *Appl. Phys. Lett.* 72, 2689 (**1998**).
23. J. Stöhr, NEXAFS spectroscopy, Spring Series in Surface Sciences, Springer-Verlag, Berlin, New York (**1992**), Vol. 25.
24. C. H. Chen and J. Shi, *Coord. Chem. Rev.* 171, 161 (**1998**).

Received: 16 July 2009. Accepted: 25 February 2010.